

Residual stress evaluation of multilayer viscoelastic composites using guided wave and electromechanical impedance signal feature variations

Houfu Jiang^a, Yanfeng Shen^{*a}, and Tao Zhang^{b, c}

^aUniversity of Michigan-Shanghai Jiao Tong University Joint Institute, Shanghai Jiao Tong University, Shanghai, 200240, China; ^bCollege of Aerospace Science and Engineering, National University of Defense Technology, Changsha, 410073, China; ^cThe 41st Institute of CASIC, Hohhot, 010010, China

ABSTRACT

Residual stresses, mainly generated by mechanical processing and strengthening approaches, are known to impose significant influence on the performance of industrial structures. They usually exist as an undesirable source of fractures and failures. Furthermore, the nondestructive evaluation and calibration of residual stresses in the depth direction always stays a significant issue, especially for multilayer viscoelastic composites. Thus, this paper proposes the advancement of residual stress evaluation technology by detecting the variation of guided wave signal and impedance features under different stress conditions. The target structure for nondestructive evaluation task is a typical multilayer, viscoelastic composite shell of a solid rocket motor. By carrying out an in-depth theoretical analysis with Finite Element Modeling (FEM), the sensing sensitivity of the probing ultrasonic wave characteristics are studied systematically. To monitor the residual stress state, a theoretical model is established by considering the stress gradient in each layer, indicating the current stress condition inside the testing object. Consequently, via the comprehensive consideration of transducer dimensions, center frequency, the most effective residual stress monitoring setup is established and the sensing signals are recorded by piezoelectric wafer active sensors (PWAS) placing on the object. Finally, different values of prestress are applied to the object, while the nonlinear constitutive law of the layered materials is implemented. The pattern between the sensing signal and the residual stress state is identified. Simulation results show that significant nonlinear features such as higher harmonic generation are fully captured, which are related to the prestress conditions. The amplitude of sensing signals could provide indicative information for evaluating the residual stress state based on the acoustoelastic effects. The amplitude and the peak shift of the impedance spectra are investigated to quantify the residual stress state. The findings of this research possess superb application potential for the evaluation of residual stresses in multilayer composites for enhancing manufacturing quality and avoiding unexpected failures in solid rocket motor industry. This paper finishes with summary, concluding remarks, and suggestions for future work.

Keywords: residual stress evaluation, nondestructive testing, ultrasonics, acoustoelasticity, composite structures

1. INTRODUCTION

Residual stress is a phenomenon that occurs in materials when they are subjected to external forces or heat treatments, resulting in internal stresses that remain in the material even after the external force or treatment is removed. Residual stress can be caused by a variety of factors, including manufacturing processes such as casting, welding, or machining, as well as thermal or mechanical loading during usage. It can also arise from changes in temperature or humidity that cause differential expansion or contraction within a material [1]. These internal stresses can have a significant impact on the mechanical, physical, and chemical properties of the material, and can lead to premature failure or deformation under certain conditions [2]. Therefore, understanding residual stress status and its effects is crucial for ensuring the integrity and longevity of materials in various applications, from aerospace and automotive engineering to construction and biomedical implants.

To this end, researchers have developed various techniques for measuring and characterizing residual stresses [3, 4]. The measurement of residual stress can be performed using various techniques categorized into destructive and nondestructive methods. Destructive methods include contour, slitting and hole drilling and nondestructive methods contains X-ray diffraction, neutron diffraction, synchrotron radiation, magnetic and ultrasonic methods [5-10]. Each technique has its own

advantages and limitations, and the choice of technique depends on the application, material, and size of the component under investigation. The accuracy and reliability of the measurement technique are critical for the interpretation of the residual stress distribution and its effects on the material behavior [11]. The evaluation of residual stress has been the subject of numerous studies and research efforts in various fields of engineering and materials science. In recent years, significant progress has been made in the development of new measurement techniques and the understanding of the physical mechanisms underlying the generation and relaxation of residual stress [12]. This has led to the development of new models and numerical simulations for the prediction and control of residual stress in complex engineering systems. However, destructive methods can cause irreversible damage to the material, while some others are only applicable to specific materials. Therefore, nondestructive testing methods are desired and widely investigated. And ultrasonics methods can reach the deepest zone into the material.

Among numerous residual stress testing methods, ultrasonic methods have emerged as a promising non-destructive technique for evaluating residual stresses in a wide range of materials, including metals, composites, and ceramics. Numerous studies have been conducted to refine and improve the accuracy and reliability of ultrasonic methods for residual stress evaluation. For example, Jiao et al. [13] proposed a method based on Lamb waves to measure the residual stresses in a steel plate, while Qozum et al. [14] developed a method based on longitudinal waves for the same purpose. Moreover, some studies have focused on the development of new algorithms and signal processing techniques for enhancing the accuracy and sensitivity of ultrasonic methods for residual stress evaluation. Lim and Sohn [15] presented the development of an online stress monitoring technique based on Lamb-wave measurements and a convolutional neural network for metallic plate-like structures under static and dynamic loadings. Kim et al. [16] developed a stress-sensing method for a pressurized vessel based on subsurface longitudinal waves. Overall, the use of ultrasonic methods for residual stress evaluation holds great promise for improving the safety and reliability of engineering structures and components.

The ultrasonic method for stress measurement is based on acoustoelastic theory, which is a well-established and widely used technique. Acoustoelastic theory is based on the principle that the propagation of ultrasonic waves in a stressed material is influenced by the presence of residual stresses, resulting in measurable changes in the velocity and attenuation of the waves [17]. By analyzing the changes in ultrasonic wave parameters, acoustoelastic theory can provide information about the magnitude, distribution, and orientation of residual stresses in a material. In recent years, there has been significant progress in the development of acoustoelastic techniques for residual stress evaluation, including experimental, theoretical, and numerical approaches [18]. This technique has been extensively studied and applied in various fields such as aerospace, automotive, manufacturing, and civil engineering [19, 20]. In this method, the ultrasonic waves are generated using a transducer and are transmitted through the material under investigation. The change in the velocity of the waves is detected and the time of flight (TOF) of sensing signals is analyzed to determine the residual stresses. These advancements have led to a better understanding of the underlying physics, improved measurement accuracy, and expanded application areas. However, detecting residual stresses in viscoelastic composites can be a challenging task due to the anisotropic and highly attenuating nature of these materials. Viscoelastic composites are known for their time-dependent mechanical behavior, which can cause the residual stress to relax over time, making it difficult to measure accurately. Additionally, the presence of viscoelasticity can cause stress to be redistributed throughout the material, leading to non-uniform stress distributions.

Apart from the ultrasonic method, another innovative approach for residual stress evaluation is the use of Electro-Mechanical Impedance Spectroscopy (EMIS). This technique involves applying an alternating signal to piezoelectric sensors attached to the material surface, subsequently measuring the resulting mechanical impedance, which can be utilized for various application conditions, such as fatigue crack monitoring [21], entire torque range monitoring of bolted joints [22] and comprehensive monitoring of carbon fiber reinforced composite laminates [23]. According to Park et al. [24], EMI spectroscopy is highly sensitive to even minor changes in material properties, including stress and strain states. Bhalla and Soh [25] further emphasize its effectiveness, noting its non-destructive nature and the ability to provide real-time monitoring of structural health. This method's accuracy and reliability in detecting residual stresses and predicting potential structural failures are pivotal, and are widely used for damage detection in industrial fields [26-29]. These studies collectively highlight the potential of EMIS as a powerful tool in the field of residual stress evaluation. However, detecting residual stresses in viscoelastic composites can be a challenging task due to the anisotropic and highly attenuating nature of these materials. Viscoelastic composites are known for their time-dependent mechanical behavior, which can cause the residual stress to relax over time, making it difficult to measure accurately. Additionally, the presence of viscoelasticity can cause stress to be redistributed throughout the material, leading to non-uniform stress distributions.

To overcome these challenges, this paper further develops the residual stress evaluation technology, utilizing the ultrasonic acoustoelastic theory by detecting the variation of nonlinear response and EMIS method by investigating the impedance amplitude peak shift under different stress and temperature conditions. The target structure for nondestructive evaluation task is a typical multilayer, viscoelastic composite shell of a solid rocket motor. Under various situations, the fundamental frequency amplitude response and the impedance peak of each case shows a meaningful pattern which provides indicative information about current residual stress state inside the material. This paper starts with the implement of the nonlinear constitutive law to the material numerical model for realization of acoustoelastic effect, followed by the method mechanism discussion. A general Finite Element Model (FEM) is established to verify the feasibility of the acoustoelastic method. Finally, a series of experiments is conducted to demonstrate the pattern of indicative index for various levels of residual stresses under different temperature conditions.

2. ACOUSTOELASTIC THEORY INTRODUCTION AND NONLINEAR CONSTITUTIVE RELATIONSHIP IMPLEMENTATION

The acoustoelastic effect is the variation of the sound velocity of an elastic material under the action of an initial static stress field, which stems from the intrinsic nonlinear relationship between the mechanical stress and the finite strain in a continuous material. In classical linear elasticity theory, most small deformations of elastic materials can be described by a linear relationship between the applied stress and the resulting strain. This relationship is often referred to as the generalized Hooke's law. The theory of linear elasticity involves a first-order elastic constant that produces constant longitudinal and shear acoustic velocities in elastic materials, independent of the applied stress. The acoustoelastic effect, on the other hand, involves higher-order expansions of the constitutive law between the applied stress and the resulting strain, which produces longitudinal and shear sound velocities that depend on the stress state of the material. The nonlinear constitutive law is particularly important in the analysis of materials that undergo large deformations, such as rubber, polymers, and biological tissues. The combination of acoustoelastic theory and nonlinear constitutive law has been used to develop advanced methods for material characterization and non-destructive testing. By measuring the acoustic waves propagating through a material and analyzing their interaction with the material's nonlinear properties, it is possible to obtain information about its elastic and mechanical properties. This has important applications in fields such as aerospace, automotive, and biomedical engineering, where the accurate characterization of materials is essential for the design of safe and reliable structures and devices.

For the purpose of numerically implementing the nonlinear constitutive law of the material, 100 stress-strain points were entered for each material using the MISO command through ANSYS finite element software and applied for large strain analysis. To reduce the workload of inputting material parameters and to make the subsequent analysis easier and smoother, MATLAB was used in conjunction with ANSYS software, and a txt file of 100 stress-strain points was prepared using MATLAB and the contents were copied into the ANSYS APDL command stream file. In the process of studying the input method of nonlinear constitutive relations in ANSYS, the fundamental parabolic equation was applied to the description of nonlinear elastic parameters. To check whether the material has been assigned with the required nonlinear constitutive relationship, a simple tensile test model was created in ANSYS for a quick and brief verification, as shown in Figure 1. Twenty different stresses were applied to the numerical bar specimen and the corresponding strains were obtained. After recording the stress-strain data and comparing the simulation results with the input data from ANSYS, the structural response was found to be in good agreement with the input data, as shown in Figure 2, indicating that the material was successfully endowed with nonlinear elastic parameters. In the following analysis, all materials were able to possess variable modulus of elasticity depending on the stress status.



Figure 1. Simple tensile test model for the verification of nonlinear constitutive relations

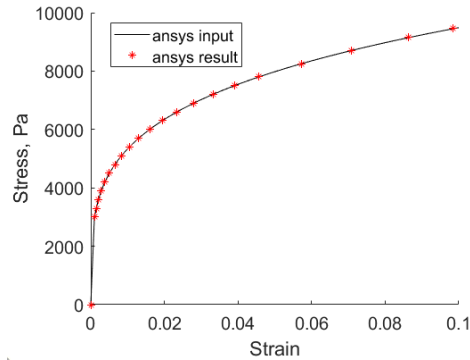


Figure 2. Input and verification on the numerical implication of nonlinear constitutive relations

3. NUMERICAL INVESTIGATION OF ZERO-STRESS AND PRESTRESS CIRCUMSTANCES

In order to develop an in-depth understanding of the residual stress evaluation method, the first step starts with a numerical multi-layer material model. The 2D plane-strain model was constructed in ANSYS to realize the simplification of the 3D complex model and save the calculation time. Therefore, the analysis with a multilayer material model with zero pre-stress was investigated. The finite element model of the multilayer material is shown in Figure 3, with a length of 200mm, divided into a carbon fiber layer (5mm) and a viscoelastic material layer (30mm). Two Piezoelectric Wafer Active Sensors (PWAS) were placed at the top, which realizes the process of a pitch-catch active sensing, and the distance between sensors was 100mm. The model embraced non-reflective boundaries on both ends, for absorbing reflections. The single-side non-reflective boundary was 50 mm long, and the mesh density becomes smaller as its distance from the model body increased, and the damping coefficient increased. In the propellant layer, the model was designed to have a fixed grid density in the upper half of the model, and the element size in the lower half of the propellant layer gradually increased as it extended vertically downward. The reason for this design is to focus on the relationship between the interface waves and the residual stresses, while the amplitude of the waves received by the lower propellant layer kept a weak amplitude due to attenuation and an actual thick body layout. Therefore, in order to increase the computational efficiency, a design with varying mesh density was used. As in the single-layer material analysis, a 10-count 300 kHz Hanning window modulated sine tone burst signal with an amplitude of 200 Vpp was used as the excitation signal. At the receiver, signals were recorded, and comparing the situations with and without prestress by plotting the temporal signals together, it can be observed that the fundamental frequency amplitude of the signals after FFT analysis reveals an increasing pattern. Furthermore, as the applied prestress increases, the amplitude of the second harmonic also increases, as shown in Figure 4. This indicates a change in ultrasonic characteristics and the capture of nonlinear ultrasonic phenomena, suggesting the manifestation of acoustoelastic effects in this analysis. The application of displacement load alters the material's constitutive relationship, resulting in changes in the constitutive range and the generation of nonlinear signal characteristics, thus indicating the potential of this method as a basis for assessing residual stress states. Therefore, numerous stress-condition-sensitive features are worth exploring during the experimental process, enabling a more effective inference of stress patterns for assessment as well as to enhance evaluation sensitivity and accuracy.

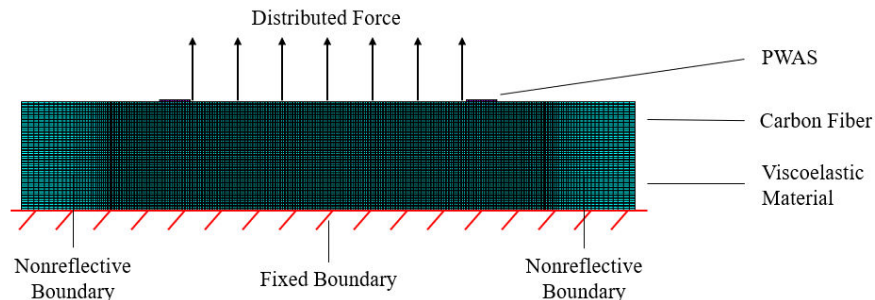


Figure 3. Numerical model illustration of multilayer composite material in 2D

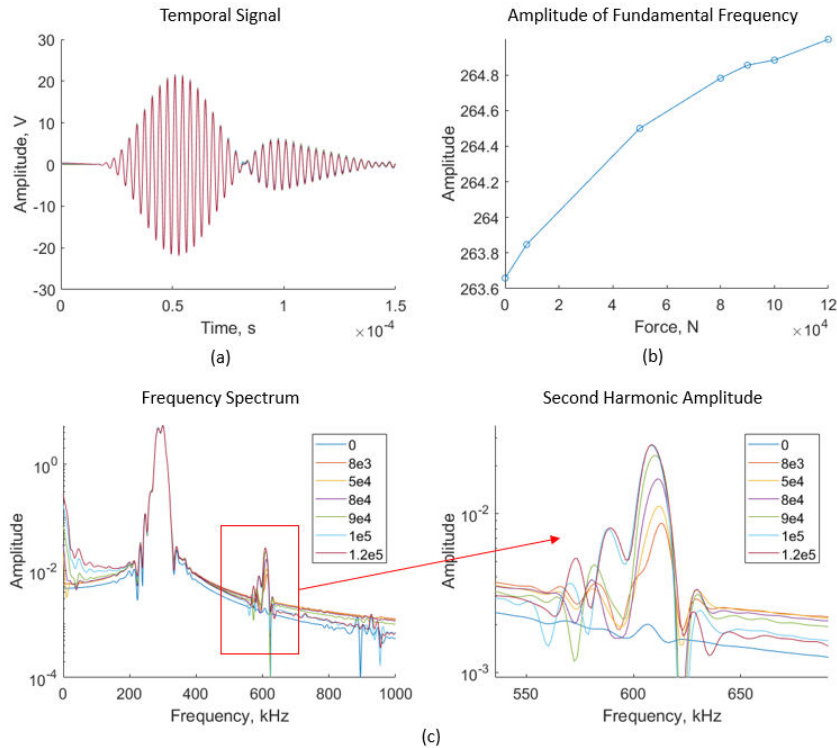


Figure 4. (a) PWAS receiver signal in temporal domain; (b) Amplitude trend of fundamental frequency in frequency domain after FFT analysis versus different pre-force value; (c) Second harmonic amplitudes based on various pre-force applied on the numerical model

4. EXPERIMENTAL DEMONSTRATION OF RESIDUAL STRESS EVALUATION

4.1 Specimen and fixture preparation

The simulation results have shown that the residual stress evaluation method is valid and effective. However, the appearance of multiple wave packets becomes the key problem of signal analysis of multilayer composite materials, which leads to the complicated receiving signal. Therefore, the frequency that is most sensitive to the stress state and has the least number of modes should be identified to facilitate the analysis. Consequently, to investigate the radial principal stress, i.e., the stress state in the z-direction, it is necessary to design the specimen size and style, as illustrated in Figure 5. The dimensions of the carbon fiber layer are 200 mm*200 mm*5 mm, bonded to the rubber layer using structural adhesive. The steel plate dimensions are also 200 mm*200 mm*5 mm, with a width of 28 mm, inserted from the rubber end and connected to a specific fixture. There are 8 through-holes in the carbon fiber and metal plate for fixation onto the fixture to apply tensile-compressive loads. The rubber bottom has 6 through-holes, clamped in the same manner as under circumferential stress conditions. The PWAS layout remains unchanged, placed on the carbon fiber surface, with the effective detection distance of 100 mm, catering to the needs for detecting more concentrated area stresses. By connecting the specimen to an MTS tensile testing machine using the fixture, it becomes possible to apply tensile-compressive loads between the carbon fiber and rubber layers, characterizing the radial stress experienced by the engine shell.

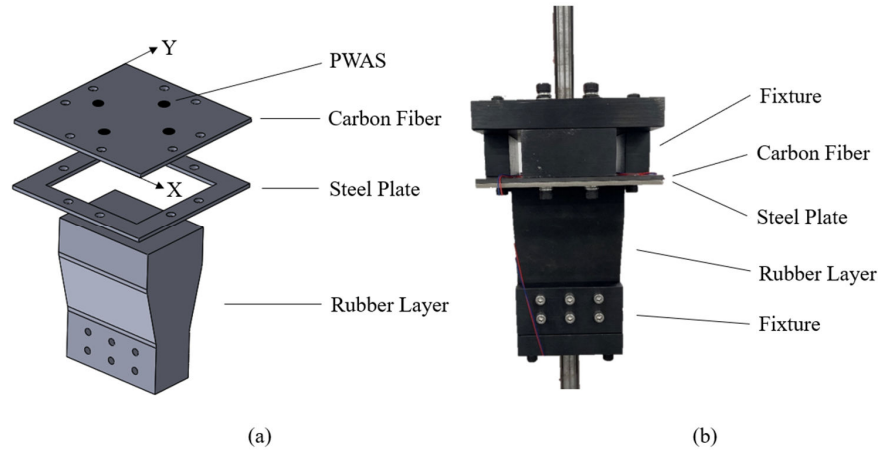


Figure 5. (a) Residual stress evaluation specimen design with SolidWorks; (b) Actual specimen with particular fixture

4.2 Guided wave active sensing experiments and results

With the help of the function generator and the amplifier, the tuning process was conducted in order to find the most sensitive frequency. Using a 20-count Hanning window modulated sine tone burst signal for excitation, it was observed that in the x-direction, three peaks were present within the frequency range of 200 kHz to 360 kHz, whereas in the y-direction, only one peak was detected within the frequency range of 220 kHz to 320 kHz. This discrepancy can be attributed to slight structural differences between the two directions, where reflections of waves in the y-direction could affect the reception signal of the sensor. However, both directions exhibited relatively consistent operating frequencies, with a frequency of 290 kHz. Furthermore, examination of the received signals corresponding to the maximum amplitudes revealed a relatively singular guided wave mode, with minimal occurrence of other modes. Therefore, signals received at this frequency are deemed the most sensitive and convenient to analysis.

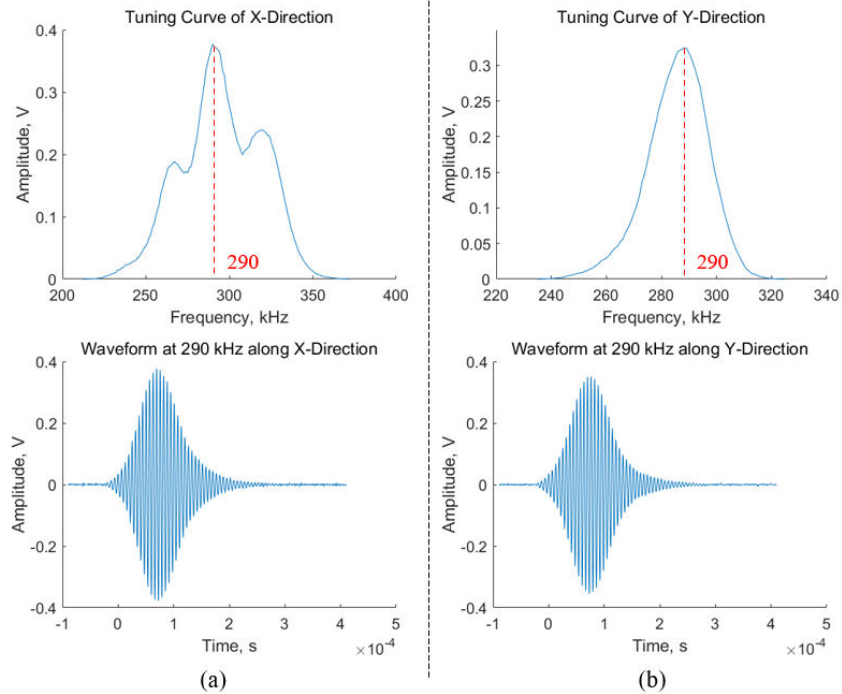


Figure 6. Tuning results and corresponding waveform at the most sensitive frequency in (a) X-direction; (b) Y-direction

The main experimental apparatus of the system was comprised of an NI PXIe-1071 high-performance waveform generator, Aigtek ATA-4014 power amplifier, KH Model 7602M power amplifier, a temperature chamber, MTS machine and a computer, as depicted in Figure 7. The NI system is utilized for signal excitation, reception, and subsequent post-processing tasks. The power amplifiers serve to increase the amplitude of the excitation signals, generating signals with broader coverage and higher intensity. The computer is employed to integrate LabVIEW software with the NI system, facilitating a comprehensive stress calibration and testing process. Initially, the NI system transmits the pre-set signals to the two power amplifiers, which amplify the signals before they are input to PWAS. The tensile test machine was used to provide tensile stress on the specimen, covering 0.05 MPa to 1 MPa, thus characterizing the residual stresses present in the specimen, while the temperature chamber was utilized to impose environmental temperature variations, covering -20°C to 70°C. The received signals are then fed back into the NI system for post-processing, enabling the extraction of characteristic values relevant to the stress state under different temperature and stress load conditions. This contributes to inferring the stress levels within the specimen.

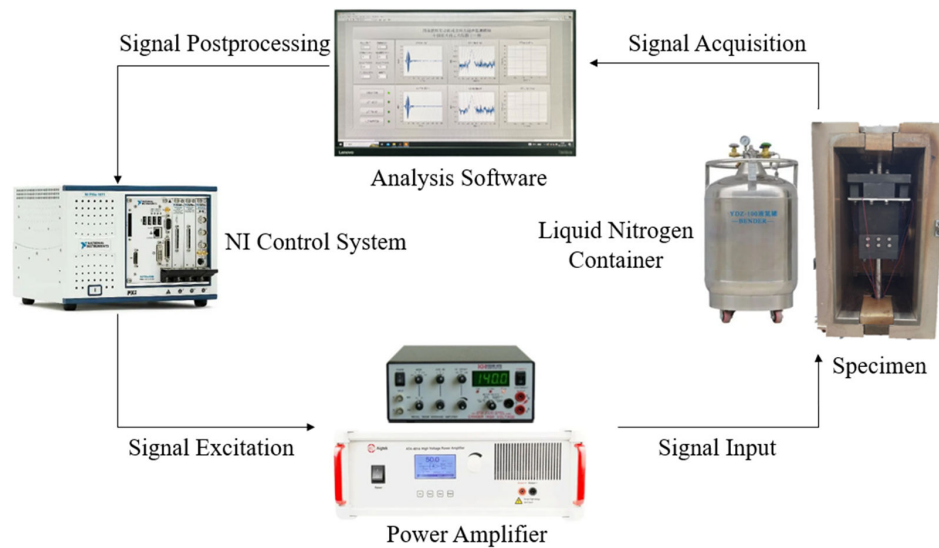


Figure 7. Experimental setup of residual stress evaluation under different stress and temperature conditions

Based on the designed specimen, stress evaluation experiment was conducted at room temperature. However, it was terminated at approximately 0.15MPa due to the detachment of the bonding interface between the carbon fiber layer and the rubber layer. Therefore, based on the results of finite element model analysis, fundamental frequency amplitude analysis was employed to establish its relationship with stress variations and explore the patterns between them. FFT analysis was performed on the received signals, and the maximum fundamental frequency amplitude was extracted to elucidate its relationship with stress states, as illustrated in Figure 8. Consistent with the finite element simulation results, under a temperature of 40°C, the fundamental frequency amplitude exhibited a monotonic linear increase with changes in stress states. Hence, it can be prioritized as a characteristic value for stress state assessment. Subsequently, a three-dimensional surface plot of the fundamental frequency amplitude against all temperature and stress conditions was generated to visually observe the intrinsic relationship between stress states and the fundamental frequency amplitude. It can be concluded that the fundamental frequency amplitudes in both directions exhibited a significant upward trend with increasing stress and temperature, which is essential for stress assessment. This phenomenon enables more accurate real-time inference of stress states, and the current stress state can be determined through linear interpolation of temperature and fundamental frequency amplitude values.

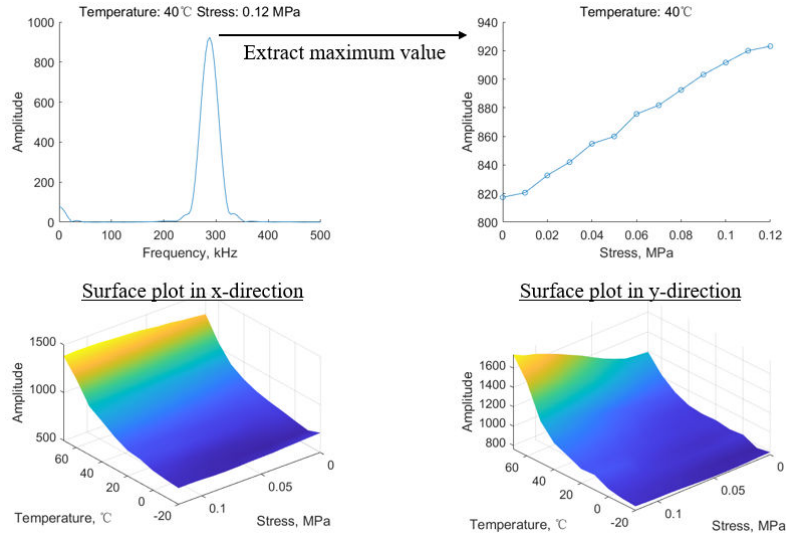


Figure 8. Fundamental frequency amplitude extraction and surface plot against all temperature and stress conditions

4.3 EMI active sensing and results

The identified patterns are based on a pitch-catch experimental design, which requires the use of four PWASs during each experiment, which leads to a relatively high testing complexity. Hence, another stress testing method based on electromechanical impedance spectroscopy (EMIS) techniques is also explored. The advantage of this method lies in the use of a single PWAS serving as both the transmitter and receiver, providing effective detection information based on the impedance spectrum obtained. This method is convenient to operate and finds widespread application in damage detection in the industrial sector. Therefore, the electromechanical impedance method is also considered an effective approach for measuring residual stress. The experimental setup, as depicted in Figure 9, includes an impedance analyzer, analysis software, industrial computer, tensile testing machine, specimen, and temperature chamber. Analysis of the impedance spectra obtained from the analyzer at room temperature reveals a clear trend of increasing maximum impedance amplitude with increasing stress, as illustrated in Figure 10. Meanwhile, it demonstrates the variation trend of the maximum impedance value with stress and its root mean square deviation (RMSD), indicating the sensitivity of impedance values and RMSD to stress changes, thus validating the electromechanical impedance method as a basis for stress assessment. Further experiments under different temperature conditions reveal a three-dimensional surface plot of the maximum impedance amplitude and corresponding frequency against stress variations, demonstrating its sensitive response to stress changes. Additionally, it is observed that at the maximum stress point at 20°C, both impedance amplitude and frequency undergo abrupt changes. Moreover, a notable change in the relationship between impedance and stress is observed after 20°C. Observation of the specimen indicates partial delamination between the carbon fiber layer and the rubber layer, further demonstrating that this method is not only sensitive to stress changes but also capable of detecting delamination phenomena in the specimen.

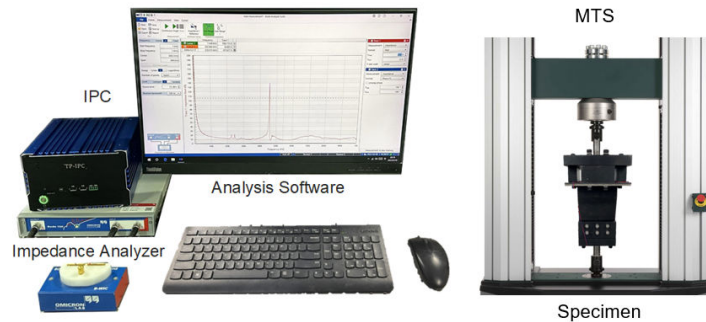


Figure 9. Experimental setup of residual stress evaluation based on EMIS method

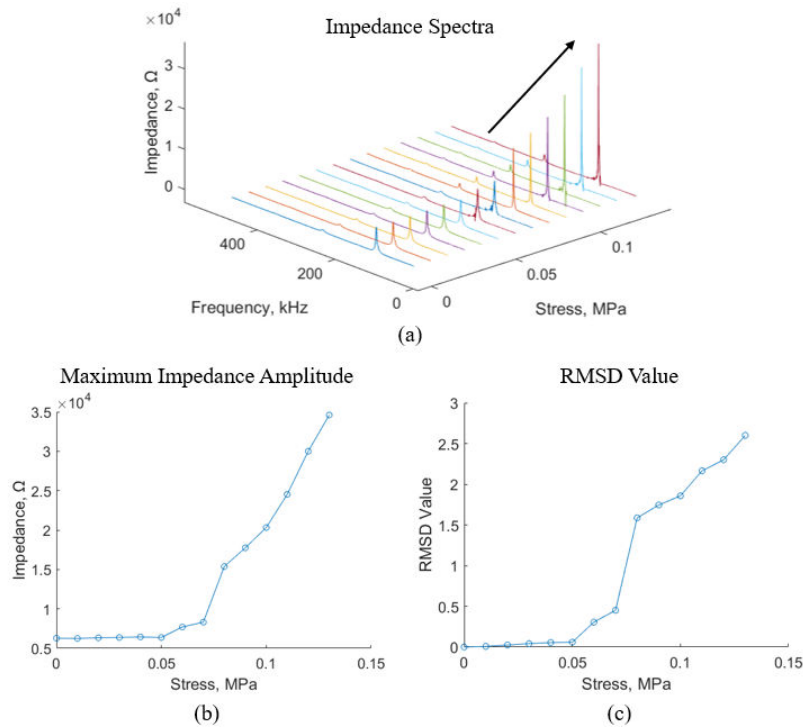


Figure 10. (a) Impedance spectra obtained based on various stress state at room temperature; (b) Maximum impedance amplitude variation trend against applied stress value; (c) RMSD value changing pattern versus prestress level

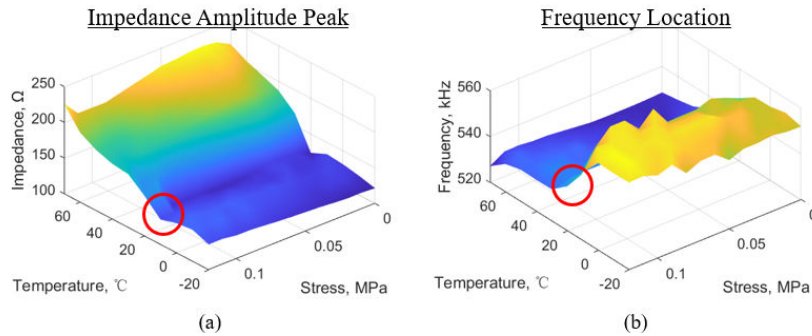


Figure 11. Surface plot against all temperature and stress conditions based on the features of (a) impedance amplitude peak and (b) corresponding frequency location

Based on the experimental results mentioned above, all the stress calibration data have been collected. Stress state testing will be conducted based on the fundamental frequency amplitude and impedance amplitude. The calibration files will be read and linear interpolation will be applied to infer the stress state. The calibration results consist of a 13×10 matrix, containing the fundamental frequency amplitude and impedance values at each temperature and stress state, which are used for linear interpolation to calculate the stress state in reverse. Therefore, stress inversion will be performed on the original specimens by testing under different temperatures and stress conditions to determine the accuracy of this method. Using a temperature chamber to control the environment at a certain temperature, the specimens will be stretched to random stress states using a tensile testing machine. After stabilization, the actual stress will be measured using this method. For instance, when the tensile force is zero, the measured average stress is -0.0073 MPa, which corresponds well with the actual stress. As the tensile force changes to 1200N and 3000N, the corresponding stresses are 0.03 MPa and 0.0075 MPa, respectively. The actual measured average stresses are 0.03125 MPa and 0.07265 MPa, with relatively small errors.

Multiple stress tests were conducted, and their errors were calculated, as shown in Table 1. It can be observed that the errors range from 3% to 8.5% in the tests, with some of the errors stemming from fluctuations in the tensile force provided by the tensile testing machine, which does not always provide the precise desired force level.

Table 1. Stress evaluation results with corresponding errors based on random temperature and applied stress

Temperature/°C	Applied Force/N	Actual Stress/MPa	Measured Stress/MPa	Error
50	0	0	-0.0073	NaN
50	1200	0.03	0.03125	4.17%
50	3000	0.075	0.07265	3.53%
60	0	0	-0.0045	NaN
60	1000	0.025	0.02712	8.48%
60	2400	0.06	0.06489	8.15%

5. CONCLUDING REMARKS

This paper presented a residual stress evaluation method for multilayer viscoelastic composite materials based on acoustoelastic effect and electromechanical impedance spectroscopy (EMIS). It was found that the nonlinear constitutive relations were successfully loaded on each layer of the material and the programmable stress-strain curves were obtained, allowing the material parameters to be changed arbitrarily according to the actual working conditions. By comparing the received signals from the sensors and their spectra, it was found that under the loading of stresses and considering the nonlinear constitutive relation, the fundamental frequency amplitude and impedance peak revealed a significant pattern which became an important basis for assessing the stress state. Tuning experiments were conducted where the particular frequency with highest sensitivity and lowest complexity was identified to facilitate the analysis. Aiming at the characterization of residual stresses at the bonding interfaces, the correlation between stress state and the fundamental frequency amplitude due to acoustoelastic effect was employed to form an effective and comprehensive residual stress characterization technique. Testing results indicated that the stress applied on the specimen was successfully measured with tiny errors. Additionally, the introduction of the electromechanical impedance method allows for the assessment of stress states using multiple approaches, resulting in a more precise estimation of the average stress level, which would provide technical support to guarantee the safety and integrity of key engine structures. These findings not only validate the feasibility of the methodology but also demonstrate a high level of accuracy and reliability in practical applications.

ACKNOWLEDGEMENTS

The supports from the National Natural Science Foundation of China (Contract Numbers 51975357); the support from Shanghai Rising-star Program (Contract Number 21QA1405100) are thankfully acknowledged.

REFERENCES

- [1] P. J. Withers, "Residual stress and its role in failure," *Reports on Progress in Physics*, vol. 70, no. 12, p. 2211, 2007/11/27 2007, doi: 10.1088/0034-4885/70/12/R04.
- [2] R. Bullough, V. R. Green, B. Tomkins, R. Wilson, and J. B. Wintle, "A review of methods and applications of reliability analysis for structural integrity assessment of UK nuclear plant," *International Journal of Pressure Vessels and Piping*, vol. 76, no. 13, pp. 909-919, 1999/11/01/ 1999, doi: [https://doi.org/10.1016/S0308-0161\(99\)00069-1](https://doi.org/10.1016/S0308-0161(99)00069-1).
- [3] N. S. Rossini, M. Dassisti, K. Y. Benyounis, and A. G. Olabi, "Methods of measuring residual stresses in components," *Materials & Design*, vol. 35, pp. 572-588, 2012/03/01/ 2012, doi: <https://doi.org/10.1016/j.matdes.2011.08.022>.

- [4] P. J. Withers, M. Turski, L. Edwards, P. J. Bouchard, and D. J. Buttle, "Recent advances in residual stress measurement," *International Journal of Pressure Vessels and Piping*, vol. 85, no. 3, pp. 118-127, 2008/03/01/ 2008, doi: <https://doi.org/10.1016/j.ijpvp.2007.10.007>.
- [5] X. Zhu and F. Lanza di Scalea, "Thermal Stress Measurement in Continuous Welded Rails Using the Hole-Drilling Method," *Experimental Mechanics*, vol. 57, no. 1, pp. 165-178, 2017/01/01 2017, doi: 10.1007/s11340-016-0204-8.
- [6] C. Xu, H. Li, J. Wang, Q. Pan, and D. Xiao, "Ultrasonic shear and longitudinal wave testing method of residual stress," *Acta Acustica*, vol. 42, no. 2, pp. 195-204, 2017.
- [7] A. J. Allen, M. T. Hutchings, C. G. Windsor, and C. Andreani, "Neutron diffraction methods for the study of residual stress fields," *Advances in Physics*, vol. 34, no. 4, pp. 445-473, 1985/01/01 1985, doi: 10.1080/00018738500101791.
- [8] C. H. Ma, J. H. Huang, and H. Chen, "Residual stress measurement in textured thin film by grazing-incidence X-ray diffraction," *Thin Solid Films*, vol. 418, no. 2, pp. 73-78, 2002/10/15/ 2002, doi: [https://doi.org/10.1016/S0040-6090\(02\)00680-6](https://doi.org/10.1016/S0040-6090(02)00680-6).
- [9] L. Mierczak, D. C. Jiles, and G. Fantoni, "A New Method for Evaluation of Mechanical Stress Using the Reciprocal Amplitude of Magnetic Barkhausen Noise," *IEEE Transactions on Magnetics*, vol. 47, no. 2, pp. 459-465, 2011, doi: 10.1109/TMAG.2010.2091418.
- [10] A. Suárez, J. M. Amado, M. J. Tobar, A. Yáñez, E. Fraga, and M. J. Peel, "Study of residual stresses generated inside laser clad plates using FEM and diffraction of synchrotron radiation," *Surface and Coatings Technology*, vol. 204, no. 12, pp. 1983-1988, 2010/03/15/ 2010, doi: <https://doi.org/10.1016/j.surfcoat.2009.11.037>.
- [11] X. Huang, Z. Liu, and H. Xie, "Recent progress in residual stress measurement techniques," *Acta Mechanica Solida Sinica*, vol. 26, no. 6, pp. 570-583, 2013/12/01/ 2013, doi: [https://doi.org/10.1016/S0894-9166\(14\)60002-1](https://doi.org/10.1016/S0894-9166(14)60002-1).
- [12] W. Z. Zhuang and G. R. Halford, "Investigation of residual stress relaxation under cyclic load," *International Journal of Fatigue*, vol. 23, pp. 31-37, 2001/01/01/ 2001, doi: [https://doi.org/10.1016/S0142-1123\(01\)00132-3](https://doi.org/10.1016/S0142-1123(01)00132-3).
- [13] J. Jiao, L. Li, X. Gao, Q. Cheng, C. He, and B. Wu, "Application of Nonlinear Lamb Wave Mixing Method for Residual Stress Measurement in Metal Plate," *Chinese Journal of Mechanical Engineering*, vol. 36, no. 1, p. 12, 2023/01/31 2023, doi: 10.1186/s10033-023-00832-6.
- [14] H. Qozam, S. Chaki, G. Bourse, C. Robin, H. Walaszek, and P. Bouteille, "Microstructure Effect on the Lcr Elastic Wave for Welding Residual Stress Measurement," *Experimental Mechanics*, vol. 50, no. 2, pp. 179-185, 2010/02/01 2010, doi: 10.1007/s11340-009-9283-0.
- [15] H. J. Lim and H. Sohn, "Online Stress Monitoring Technique Based on Lamb-wave Measurements and a Convolutional Neural Network Under Static and Dynamic Loadings," *Experimental Mechanics*, vol. 60, no. 2, pp. 171-179, 2020/02/01 2020, doi: 10.1007/s11340-019-00546-8.
- [16] H. Kim, T. Kim, D. Morrow, and X. Jiang, "Stress Measurement of a Pressurized Vessel Using Ultrasonic Subsurface Longitudinal Wave With 1-3 Composite Transducers," *IEEE Transactions on Ultrasonics, Ferroelectrics, and Frequency Control*, vol. 67, no. 1, pp. 158-166, 2020, doi: 10.1109/TUFFC.2019.2941133.
- [17] G. C. Johnson, "Acoustoelastic theory for elastic-plastic materials," *The Journal of the Acoustical Society of America*, vol. 70, no. 2, pp. 591-595, 1981, doi: 10.1121/1.386748.
- [18] C.-S. Man and W. Y. Lu, "Towards an acoustoelastic theory for measurement of residual stress," *Journal of Elasticity*, vol. 17, no. 2, pp. 159-182, 1987/01/01 1987, doi: 10.1007/BF00043022.
- [19] W. Wang, Y. Zhang, Y. Zhou, S. Meng, and D. Chen, "Plane stress measurement of orthotropic materials using critically refracted longitudinal waves," *Ultrasonics*, vol. 94, pp. 430-437, 2019/04/01/ 2019, doi: <https://doi.org/10.1016/j.ultras.2018.03.015>.
- [20] D. Mingxi, "Cumulative second-harmonic generation accompanying nonlinear shear horizontal mode propagation in a solid plate," *Journal of Applied Physics*, vol. 84, no. 7, pp. 3500-3505, 1998, doi: 10.1063/1.368525.
- [21] R. Lu, Y. Shen, B. Zhang, and W. Xu, "Nonlinear Electro-Mechanical Impedance Spectroscopy for fatigue crack monitoring," *Mechanical Systems and Signal Processing*, vol. 184, p. 109749, 2023.
- [22] R. Lu and Y. Shen, "Entire Torque Range Monitoring of Bolted Joints Via Nonlinear Electromechanical Impedance Spectroscopy (NEMIS)," in *50th Annual Review of Progress in Quantitative Nondestructive Evaluation*, 2023, vol. 87202: American Society of Mechanical Engineers, p. V001T07A001.

- [23] R. Lu and Y. Shen, "Nonlinear Electro-Mechanical Impedance Spectroscopy for Comprehensive Monitoring of Carbon Fiber Reinforced Composite Laminates," in *ASME International Mechanical Engineering Congress and Exposition*, 2022, vol. 86625: American Society of Mechanical Engineers, p. V001T01A014.
- [24] G. Park, H. Sohn, C. R. Farrar, and D. J. Inman, "Overview of piezoelectric impedance-based health monitoring and path forward," *Shock and vibration digest*, vol. 35, no. 6, pp. 451-464, 2003.
- [25] S. Bhalla and C. K. Soh, "Electromechanical impedance modeling for adhesively bonded piezo-transducers," *Journal of intelligent material systems and structures*, vol. 15, no. 12, pp. 955-972, 2004.
- [26] J. Raju, S. Bhalla, V. Talakokula, and S. Thakur, "Industrial applications of electro-mechanical impedance technique in novel non-bonded configurations," in *Sensors and Smart Structures Technologies for Civil, Mechanical, and Aerospace Systems 2019*, 2019, vol. 10970: SPIE, pp. 44-50.
- [27] A. Miska and A. Zagari, "On Structural Damping Characteristics in the Electro-Mechanical Impedance Method," in *ASME International Mechanical Engineering Congress and Exposition*, 2021, vol. 85611: American Society of Mechanical Engineers, p. V07AT07A005.
- [28] T. Saar, O. Märtens, M. Reidla, and A. Ronk, "Chirp-based impedance spectroscopy of piezo-sensors," in *2010 12th Biennial Baltic Electronics Conference*, 2010: IEEE, pp. 339-342.
- [29] R. Lu, Y. Shen, W. Qu, and L. Xiao, "Health monitoring of high-damping viscoelastic materials using sub-resonator enriched electro-mechanical impedance signatures," *Smart Materials and Structures*, vol. 31, no. 9, p. 095046, 2022.